

THOMAS M. LILLESAND
DOUGLAS E. MEISNER
DAVID W. FRENCH
WILLIAM L. JOHNSON
University of Minnesota
St. Paul, MN 55108

Evaluation of Digital Photographic Enhancement for Dutch Elm Disease Detection*

The computer enhanced images dramatically increased the expression of subtle within-crown and between-crown color variations, but only nominally improved detection accuracy.

INTRODUCTION

THE SUCCESS of any Dutch elm disease (DED) control program is contingent upon, among other things, early and accurate detection of the disease in affected trees. Numerous studies have investigated the potential of using manual interpretation of color infrared aerial photography to

The study reported herein was aimed at assessing the utility of digitizing and enhancing vertical color infrared photography as a means of improving upon the aerial detection process. The research was conducted within the metropolitan area of Minneapolis/St. Paul, Minnesota, during 1979-80.

ABSTRACT: *Previous studies have indicated that crown morphology and within-crown color variations, rather than between-crown color differences, are principal keys to the accurate aerial detection of Dutch elm disease (DED). Because within-crown color variations often tend to be very subtle on conventional infrared photographs, microdensitometry and subsequent digital enhancement were evaluated as potential means of improving detection accuracy.*

Vertical 70-mm color infrared photographs at scales of 1:6,000 and 1:12,000 were taken on several dates over a study area containing high incidence of DED. Scanning microdensitometer data from the photographs were processed using three enhancement techniques: color contrast stretch, two-band spectral ratioing, and multiple discriminant analysis. The numerically processed data were subsequently re-converted to image form using a high resolution color film recorder. Experienced interpreters analyzed both the original imagery and the enhanced products.

The computer enhanced images dramatically increased the expression of subtle within-crown and between-crown color variations, but only nominally improved detection accuracy. Thus, the factor limiting detection from vertical photography appears to be the inconsistency, not the subtlety, in which DED is manifested as crown color variation.

detect DED. The success of these studies has been quite mixed, but generally the photographic methods have not yielded detection accuracies adequate for disease control.

* Published as Paper No. 11,529, Scientific Journal Series, Minn. Agric. Expt. Sta., St. Paul, MN 55108. Presented, in part, at the 7th International Symposium on Machine Processing of Remotely Sensed Data, West Lafayette, Indiana, June 1981.

PREVIOUS STUDIES

Attempts to use color infrared aerial photography to detect DED in Minnesota date back to 1964, when a variety of photo scales was tested as the disease first began to move into the state. These studies indicated that scales in the 1:6,000 to 1:12,000 range seemed to offer the greatest detection potential (Meyer and French, 1967). During

1967, a test was conducted using stereo 1:9,600-scale color infrared photo coverage of Bloomington, Minnesota, but with inconclusive results. A problem hampering these early tests was the general absence of the disease in the study areas investigated (French and Meyer, 1969). This certainly was not the case in later studies conducted during 1973 and thereafter.

In 1973, the community of North St. Paul was photographed using normal color film (color infrared imagery was not available for the study) and three methods of disease detection were compared: interpretation of the aerial photography, visual observation of the tree population from a helicopter, and normal ground checking by city crews. University personnel conducted concurrent intensive ground checks as a basis for comparison of the three methods. Interpretation of the 1:9,600-scale stereo coverage resulted in detection of only 49 (45 percent) of the 109 diseased elms in the study area. At the same time, a total of 381 trees were marked by the interpreter as possible cases of DED. That is, the error of *omission* was 55 percent (100 percent minus 45 percent) and that of *commission* was approximately 300 percent (381 minus 49/109). The commission error reflects trees marked on the photography as having the disease, but which are not actually diseased. The omission and commission errors for the helicopter observations were 32 percent and 10 percent, respectively. City ground crews failed to detect approximately 20 percent of the diseased trees during their normal survey. The inefficiency of the aerial technique was assumed to be due, in part, to the use of color, rather than color infrared, photography (French, 1974).

During 1975, vertical color infrared coverages at scales of 1:9,600 and 1:6,000 were tested over portions of Minneapolis. Three interpreters with varying degrees of experience analyzed the imagery. Results were again disappointing in that only 47 to 50 percent of the diseased elms present in the study area were detected by any one interpreter—irrespective of the image scale used (Fairweather *et al.*, 1978). A major problem encountered during the study was the fact that variation in color among the elms in the study area made the identification of a diseased tree on the basis of general crown color virtually impossible. Accordingly, the interpretation had to be based on morphological peculiarities and very subtle color changes *within* each crown. This form of interpretation is often very difficult to implement due to confusion between a tree crown and the ground below when both are photographed vertically. That is, such things as street surfaces, sidewalks, shrubs, and grass, which appear in the gaps of crowns, can be mistaken for crown features.

With the hope of minimizing the background

problem characterizing vertical photography, a 1976 study evaluated oblique 35-mm photography as an alternative data source for the interpretation process. In this study, exposures were made at an angle of 45° from the vertical using both color and color infrared films at various scales. The images were taken with the sun behind the camera during exposure to minimize shadow effects. This technique limited the appearance of background objects in the photographs. The approach enabled an experienced interpreter to detect 74 percent of the diseased trees in the study area from color infrared images having a center-of-frame scale of 1:8,400. Errors of commission were on the order of 57 percent (Nash *et al.*, 1977). While these results represented a substantial improvement over those of previous studies, they were preliminary* and still lower than desired for practical application to DED control management.

In contrast to the more conventional interpretation procedures, densitometric techniques for DED detection have received limited attention in previous investigations. Notable exceptions are studies reported by Stevens (1972) and Hammerschlag and Sopstyle (1975). In the former effort, whole-crown spectral density measurements were obtained from color infrared photographs of healthy and diseased elms in a Madison, Wisconsin, test area. Relative density differences were noted for healthy and diseased samples, but results were inconclusive due to the use of oblique photography for the experiment and a 35-mm camera having an erratic focal plane shutter. However, Stevens' work indicated that subtle disease symptoms were potentially detectable using image density measurement.

Hammerschlag and Sopstyle tested various forms of aerial photographic detection in a Washington, D.C., test area. Among other things, they attempted to expedite detection by computing ratios of densities obtained from two images taken simultaneously in different spectral bands (reflected infrared and red). Because the resulting images were not superimposable point for point, average density readings over areas had to be compared. Possibly due to this data generalization, the two-band ratio values measured were insensitive to stress levels.

Applying microdensitometry of color infrared photography to a different shade tree problem, Lillesand *et al.* (1979) were able to use spectral density measurements to quantify decline levels in a sample of street-side maples in Syracuse, New York. Between-crown density differences proved to be a reliable indicator of relative crown vigor in this case. Because DED interpretation is based on

* Continuing research is being conducted by the third author of this article to further investigate the efficiency and cost of the oblique coverage technique.

detection of morphological peculiarities and color variations within the crown rather than measuring an average absolute crown color, a hybrid approach was developed in the current study to combine densitometry with manual photointerpretation.

STUDY APPROACH

This study was conducted in two phases. First, multirate color infrared photographs were acquired at two scales over test areas which were surveyed concurrently by field crews. A preliminary interpretation of all imagery was then made to determine which combination of film type, date, and scale photography was best for DED detection purposes. A detailed visual interpretation of this optimum data set was then performed by two experienced interpreters to establish a benchmark against which subsequent interpretations of computer enhancements could be compared.

In the study's second phase, 17 photographs covering a representative portion of the test area were digitized using a scanning microdensitometer and three forms of computer enhancement were applied to the resulting data: contrast stretch color compositing, two-band ratioing, and discriminant analysis. The numerically processed data resulting from the application of each of these procedures were subsequently re-converted to image form using a computer-controlled color film recorder. These enhanced image products were then interpreted visually and the results were compared to the interpretation of the original images.

The remainder of this article summarizes the various data acquisition and analysis procedures employed in the study, and the comparative results of interpreting the conventional and computer-enhanced images.

DATA ACQUISITION

STUDY AREA

The primary test area used in this study is an older residential St. Paul area (2.6 km²) containing a mature shade tree population consisting primarily of American elms. The site was selected because it generally represents the range of environmental conditions under which operational DED monitoring programs are operated in the Twin Cities area. Further, the site includes a number of "control" elms which have been the subject of years of intensive monitoring as part of complementary DED research conducted by the University of Minnesota Department of Plant Pathology. The entire study area was intensively surveyed by city and university field crews regularly during the 1979 growing season.

AERIAL PHOTOGRAPHY

The test area was photographed on five dates during the 1979 growing season: 3 May, 15 May,

25 June, 25 July, and 6 September. Hasselblad 500 EL motor driven cameras ($f = 80$ mm) were used to obtain the 70-mm color infrared positive transparencies (Kodak film type 2443, Wratten 15 filter). For comparison purposes, both 1:6,000 and 1:12,000 scale images were taken during the July and September missions. All photographs were obtained with a nominal 60 percent endlap to afford stereoscopic viewing, all film used was manufactured in the same emulsion batch, and step wedges were exposed on each film leader prior to processing.

The overall appearance of the various sets of imagery was quite variable. The May "leaf-off" images were used solely to locate and index each tree in the test area on a base map. The photography taken during June coincided with the incidence of severe defoliation of elms in the study area by canker worms, and was acquired shortly after a period of excessive storm damage. The September photographs, while of good photographic quality, contained long shadows due to low solar altitude. The 25 July date provided the most useful photography. Accordingly, this data set was the subject of the computer-enhanced interpretation.

INTERPRETATION OF ORIGINAL PHOTOGRAPHY

PROCEDURE

The visual interpretation process commenced with locating and indexing all street-side elms on a base map. The 1:6,000 May photography was found to be very effective for this task. In these leaf-off images, elms were readily separable from other tree species because of the elms' characteristic feather-duster shadow and dark trunk and limbs. Flowering was also taking place at the time of photography, and this added another identifying characteristic for the elms. Consequently, individual elm crowns were easily discriminated from other species on the images and could be individually referenced on a map base. Accomplishing these tasks with leaf-on images is much more difficult given overlap between crowns and the similar appearance of elms and other species.

Only street-side trees were included in the interpretation process in that ground data on yard trees were not readily obtainable for comparison. This resulted in a population of 1428 trees which were located between the streets and sidewalks in the study area.

Image interpretation was performed after field visits were made to sites of selected healthy and diseased trees for training purposes. The entire set of 1:12,000 photographs for each date was first analyzed, followed by the 1:6,000 images. All images were viewed by two trained interpreters having access to conventional monocular viewing

devices and a Bausch and Lomb Zoom 70 Stereo-scope mounted on a light table.

The general guidelines used by the interpreters for disease identification were developed during previous studies (Fairweather *et al.*, 1978). They included the following:

- Variation in color among street-side elms makes the identification of a diseased tree on the basis of the general crown color almost impossible. Therefore, crown examinations should key on morphological peculiarities and color changes *within the crown*. Crown discoloration in one portion as compared to the remainder *may be extremely subtle*.
- A stereoscope should be used to determine if what appears to be a disease symptom is actually in the crown. It is easy to mistake a street, sidewalk, or driveway showing through the crown for a crown reflectance anomaly.
- Note should be made of a crown with a tattered or shredded appearance as compared with surrounding crowns.
- Elms with foliage in distinct tufts rather than uniform full crowns should be noted, as should generally thin crowns.
- Shadows cast by a suspect tree should be studied; defoliated branches may thereby become more apparent.
- Diseased elms sometimes have foliage adhering very close to only the main limbs. In these cases the shadow will appear very thick and heavy.

Using the above interpretation guidelines, each interpreter noted all apparent diseased trees and classified them into high, medium, or low levels of interpretation confidence. After the image in-

terpretation process was completed, ground data were collected on the precise location, date of field detection, and date of removal for diseased elms. The aerial and ground data sets were then compared.

RESULTS

As previously mentioned, the July data set was found to be the most useful for disease detection. As anticipated, the 1:6,000 images were slightly more amenable to interpretation than their 1:12,000 counterparts—but both were judged acceptable by the interpreters. (A scale such as 1:10,000 would probably represent an optimum compromise between areal coverage and image detail.)

As in the previous studies, accuracies were found to be low and errors high. Table 1 lists the results of the conventional interpretation process. Table 1a gives the results for the more experienced interpreter, Table 1b for the less experienced. Note that the study population included a total of 1357 healthy trees and 71 diseased trees.

The left side of Table 1 is a matrix of photointerpreted versus ground data. The photointerpretation categories of disease existence are low confidence of interpretation (D^3), moderate confidence (D^2), and high confidence (D^1). The ground data category of "diseased" trees includes those diagnosed by city crews as having DED and removed in 1979, as well as diseased trees noted by University personnel which had not yet been marked for removal by city crews. This latter group stemmed

TABLE 1. CONVENTIONAL IMAGE INTERPRETATION RESULTS

		Ground Data		classes considered "diseased"	Accuracy	Errors	
		healthy	diseased			omission	commission
(a) Interpreter 1							
P.I. Data	healthy	1320	46	D^1	$\frac{11}{71} = 16\%$	$\frac{60}{71} = 84\%$	$\frac{3}{71} = 4\%$
	D^1	3	11	D^1, D^2	$\frac{22}{71} = 31\%$	$\frac{49}{71} = 69\%$	$\frac{12}{71} = 17\%$
	D^2	9	11	D^1, D^2, D^3	$\frac{25}{71} = 35\%$	$\frac{46}{71} = 65\%$	$\frac{37}{71} = 52\%$
	D^3	25	3				
	total:	1357	71				
(b) Interpreter 2							
P.I. Data	healthy	1120	19	D^1	$\frac{12}{71} = 17\%$	$\frac{59}{71} = 83\%$	$\frac{8}{71} = 11\%$
	D^1	8	12	D^1, D^2	$\frac{46}{71} = 65\%$	$\frac{25}{71} = 35\%$	$\frac{140}{71} = 197\%$
	D^2	132	34	D^1, D^2, D^3	$\frac{52}{71} = 73\%$	$\frac{19}{71} = 27\%$	$\frac{237}{71} = 334\%$
	D^3	97	6				
	total:	1357	71				

from an intensive resurvey of the study area early in the 1980 growing season.

The right side of Table 1 lists the photointerpretation accuracies and errors. Accuracies are given as percentages of interpreter-identified versus ground-verified diseased trees. Errors of omission are simply the complements of the accuracy values. Errors of commission indicate the number of healthy trees (by ground designation) which were mistakenly classified as diseased by the interpreters. These errors are also expressed as a percent of total diseased trees. All three quantities are expressed for three different thresholds of interpretation: on the top line, only the D^1 category (high interpreter confidence in *DED* existence) is considered as diseased. In this case, the D^2 and D^3 classes would be considered non-disease anomalies. This yields very low errors of commission, but causes many diseased trees to be omitted. The second line considers classes D^1 and D^2 to be diseased, and the bottom line considers all three interpretation confidence categories.

The two tables indicate considerable difference between the two interpreters. Interpreter 1 had a higher decision threshold, classifying a total of 62 trees as diseased, as opposed to 289 trees for Interpreter 2. As a result, Interpreter 1 had less inclination toward misclassifying healthy trees (errors of commission) but also had a greater tendency to overlook diseased trees (errors of omission). Interpreter 2 found more of the diseased trees, but at the expense of including many healthy trees.

DENSITOMETRIC PROCEDURES

DENSITY MEASUREMENT

A subset of 17 images was digitized using a modified Optronics P-1700 drum scanner operated by the Environmental Remote Sensing Center (ERSC) at the University of Wisconsin-Madison. The scanner data are expressed as density values from 0 to 3D, digitized into 256 levels. Each 70-mm frame of photography was scanned at an interval of 50 μm , yielding a grid of 1100 by 1100 pixels. Given three spectral density measurements per pixel (one for each color-sensitivity layer of the film), a total of over 3.6 million measurements were taken on each photograph. The ground area represented by each pixel was 0.3-m square for the 1:6,000 scale images, and 0.6-m square for the 1:12,000 data set.

All data processing for the enhancement procedures was performed on a CDC Cyber 172 computer system using the University of Minnesota Image Processing Software (UMIPS) developed by the Remote Sensing Laboratory. The enhanced image data sets were recorded using the Dicomed D-47 color film recorder operated by the University of Minnesota Special Interactive Computation Laboratory. Photographic positives were gener-

ated for interpretation purposes and negatives for preparation of enlargements. The various forms of enhancement used to generate these images are described below.

CONTRAST STRETCH ENHANCEMENT

While the densitometer records density values over the entire range from 0 to 3D, most of the features in a typical photograph have values within a small range of the total density scale. As a result, slight differences are often very hard to distinguish and are frequently undetectable by the human interpreter. In the contrast stretch enhancement process, the original image density values are modified such that the more frequently occurring "medium" levels occupy a larger range of image values. This makes variation in the medium tones easier to differentiate, at the expense of less differentiation in the infrequently occurring very bright or very dark features. Because the elm tree crowns tend to be of medium tone, contrast stretching enhances the tonal rendition of these features. The form of contrast stretch used in this project is called *histogram equalization* because it is based on the histogram of grey values in the image. It is performed independently on each color sensitivity layer in the image, generating three modified primary color image files. During film recording the data are composited through color filters, creating an image which enhances color variation in the medium tonal range.

RATIO IMAGES

A ratio image is derived by dividing the image density value from one film layer by the value in another layer for each pixel in the image. The resulting ratio values are then displayed as an image. This procedure tends to negate various extraneous factors that act nearly equally in each of the spectral bands under analysis. For example, from the sunlit to the shaded side of a tree crown, the image values will change considerably and this change will have no relation to the crown spectral characteristics per se. Yet if the shade reduces *both* the green and red levels approximately equally, the ratio of green to red values should remain fairly constant throughout the crown. True color changes within the crown, as opposed to overall brightness changes, will result in different ratios. In theory, the color differences should be more noticeable after removal of the extraneous brightness variations. This technique essentially attempts to screen out meaningless tonal variations caused by such factors as position within the photograph, shading, etc.

The measurement unit of density in which the densitometer data are expressed is logarithmic. As a result, ratios are computed simply by subtracting the digital values in two image layers and adding

127 (to avoid negative values). Since a ratio image is computed for a pair of film sensitivity layers, three combinations are possible: green/red, green/infrared, and red/infrared (as well as the inverse of these). We recorded ratios such that an equal reflectance in both channels appears as a medium grey, a high reflectance in one film layer relative to the other appears as white, and a high relative reflectance in the other layer appears as black. The inverse ratio images were generated by producing both positive and negative images at the film recording stage. Furthermore, the ratio data were contrast stretched with the histogram equalization technique prior to film recording.

Additional discussion of contrast stretch and ratio enhancements can be found in Lillesand and Kiefer (1979).

MULTIPLE DISCRIMINANT ANALYSIS

The principal shortcoming of the ratio technique is the limitation to two image bands in a given display. It is difficult to say which of the possible ratio combinations is optimum for the application at hand. Discriminant analysis is similar to the ratio technique except that all bands of the data are used in a single display and the values are combined using weighting factors which maximize the discriminability of the features being analyzed. The weighting factors are determined from a sample of image values from each of the two types of features to be distinguished (in this case, diseased and non-diseased elms). Statistical analysis of the two sets of values (using the two means and a pooled variance/covariance matrix) are used to compute the factors (Morrison, 1976).

When generating a discriminant image, the three spectral values for each pixel are multiplied by their corresponding coefficients and added to derive the discriminant image value. This process expressed in equation form is

$$X' = X_g C_g + X_r C_r + X_{ir} C_{ir}$$

where

X' = multiple discriminant value,

X_g, X_r, X_{ir} = original image values (green, red, IR), and

C_g, C_r, C_{ir} = discriminant coefficients for each film layer.

Using the above technique, "discriminant images" were prepared by relating image brightness to discriminant value during the film recording process.

INTERPRETATION OF ENHANCED IMAGERY

EXAMPLES OF ENHANCED IMAGERY

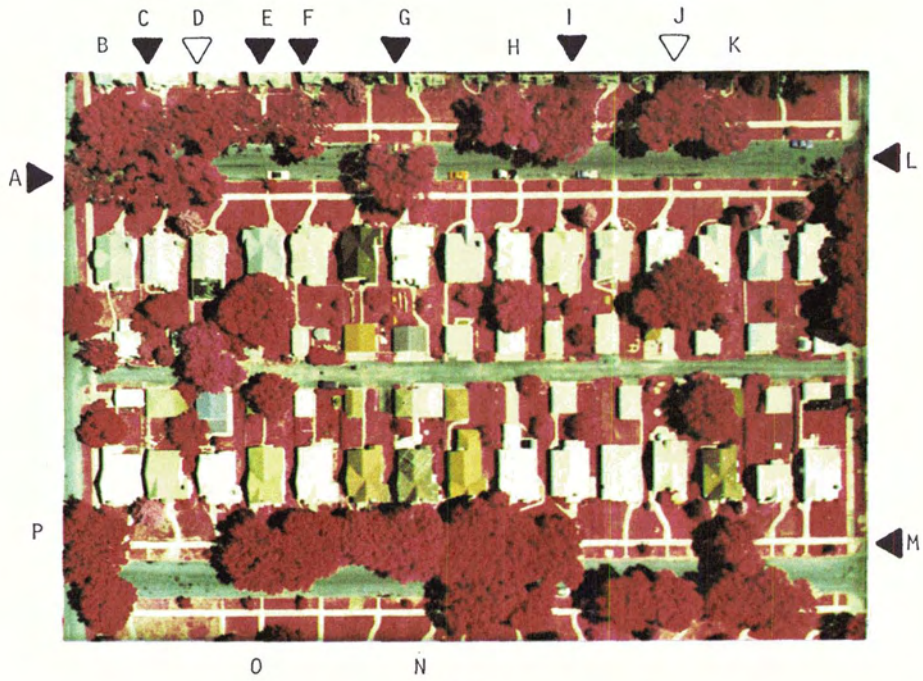
Plate 1 and Figure 1 are photographic enlargements which permit comparison of the effects of the various enhancement procedures. These

prints cover one city block which is characteristic of the study area. Examples from the 1:6,000 original scale images are shown. The scale of the enlargements is approximately 1:1,600 and they generally depict the view the interpreters had of the original images under magnification. A number of crowns have been labeled alphabetically for reference purposes. Also, the diseased tree crowns determined from the ground survey are indicated by arrows. The black arrows represent trees designated by the city crews in 1979 and removed. The outline arrows are trees found in the 1980 resurvey which were diseased but not removed in 1979.

Plate 1 is a comparison of an original 1:6,000 scale color infrared photograph to its contrast stretched counterpart. It should be noted that the detail and color fidelity is greatly reduced in all of these prints compared to the originals. Individual pixels can be seen much more clearly on the original products than in this presentation. In spite of these shortcomings, these sample images illustrate the considerable improvement in tonal information provided by the contrast stretch enhancement. For example, the color variations shown in crowns *D*, *F*, *I*, and *J* on the enhanced image are virtually undetectable on the original. The problem is that the stretch process enhances color variations in healthy crowns as well. The crowns at *O* and *P*, which are healthy trees, would probably be interpreted as diseased (in error on the enhanced image). The crown at *L* shows another deficiency of the digital imagery; the reduced spatial detail due to the scanning process makes very sparse crowns difficult to pick out. This problem was particularly acute on the 1:12,000 product. Thus, the interpreter must view both the original and the enhancement to be certain to not miss very sparse crowns.

The enlargements in Plate 1 illustrate some other general points about the appearance of diseased and healthy trees on the enhanced image. Crowns *H* and *N* appear to have considerably different color than those nearby, but the lack of within-crown variation indicates a healthy tree. Crown *I* shows the disease effect spread throughout most of the crown, whereas crown *J* shows a clump of diseased branches. Crown *K* shows essentially the same clump appearance as crown *J*, yet the tree was not judged diseased by the ground crews. The crown at *M* (up the street three houses from the corner) cannot be interpreted as having DED based on color; the irregular shape is the only indication. Yet, a similar irregularity in shape of the crown across the street from crown *D* is associated with a tree which was not classified as diseased by the ground crews. The overlapping of crowns from *A* to *F* shows the difficulty of separating closely spaced trees and the utility of preliminary interpretation of spring photography for tree identification.

Figures 1a, 1b, and 1c show the enlarged ratio



(a)

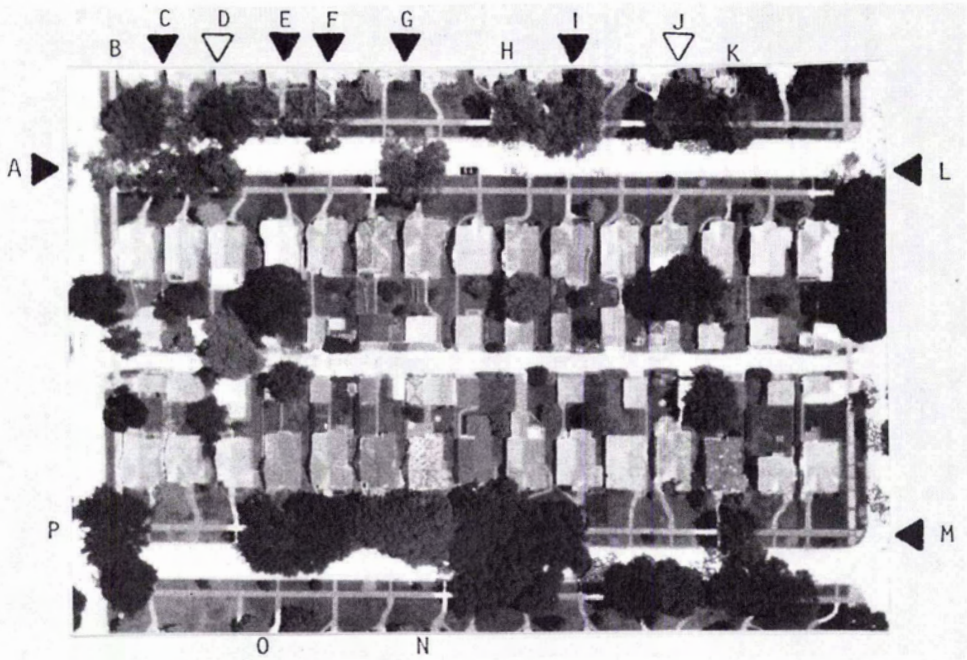


(b)

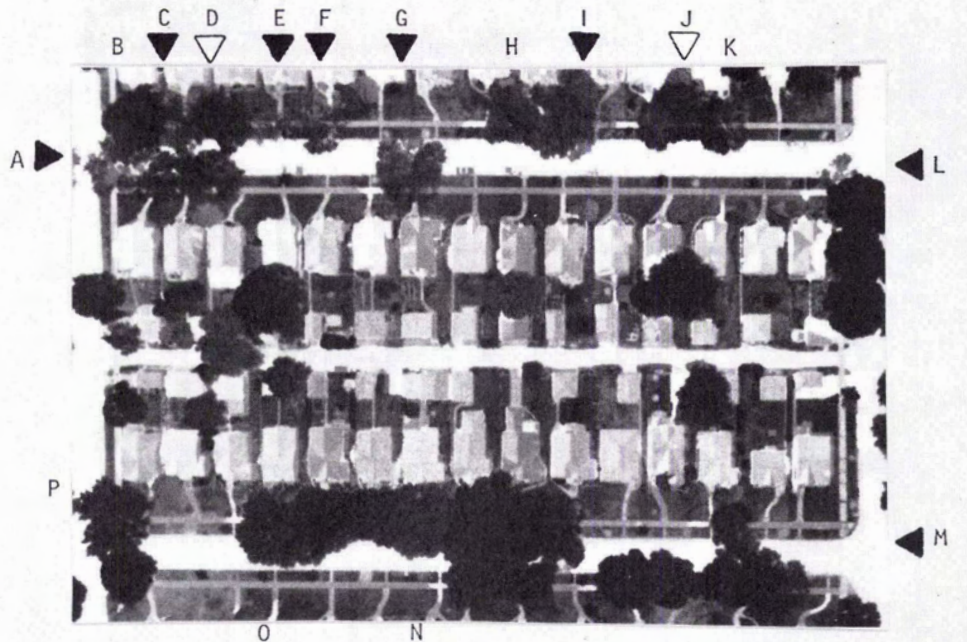
PLATE 1. Sample contrast stretched images. (a) Original photograph. (b) Contrast stretched image.

images of the same block depicted in Plate 1, and Figure 1d shows the discriminant image. These images were generated from the 1:6,000 original scale data. Note the similarity between Figures 1a,

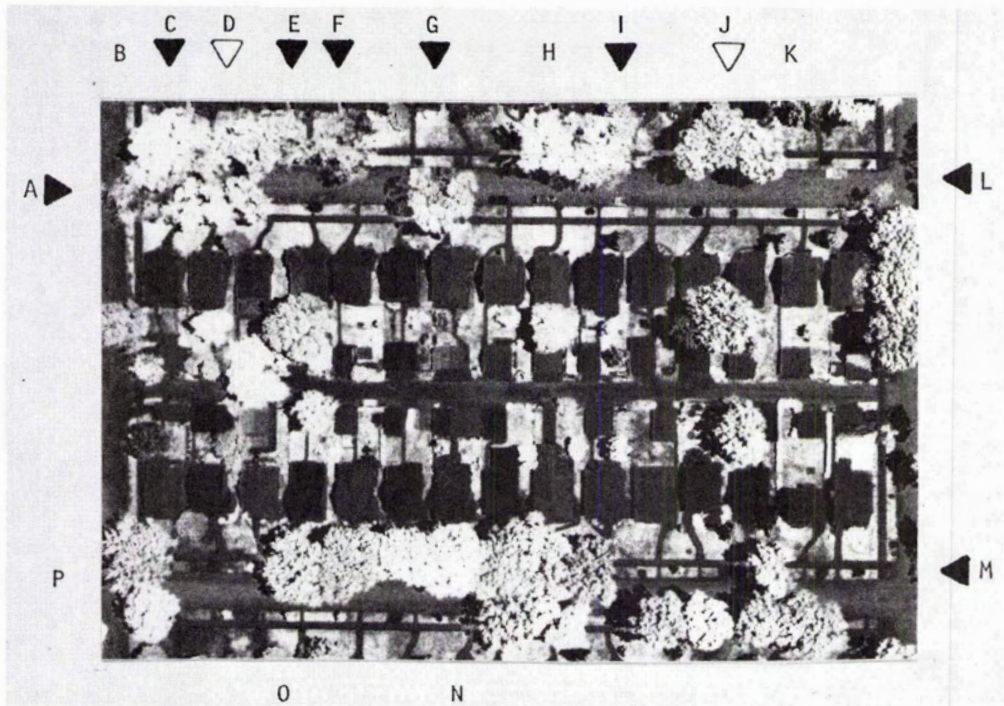
1b, and 1d. Each of these presents the healthy trees in dark tones and the diseased trees in light tones (the reversed rendition was also generated but was found to be the less interpretable). The



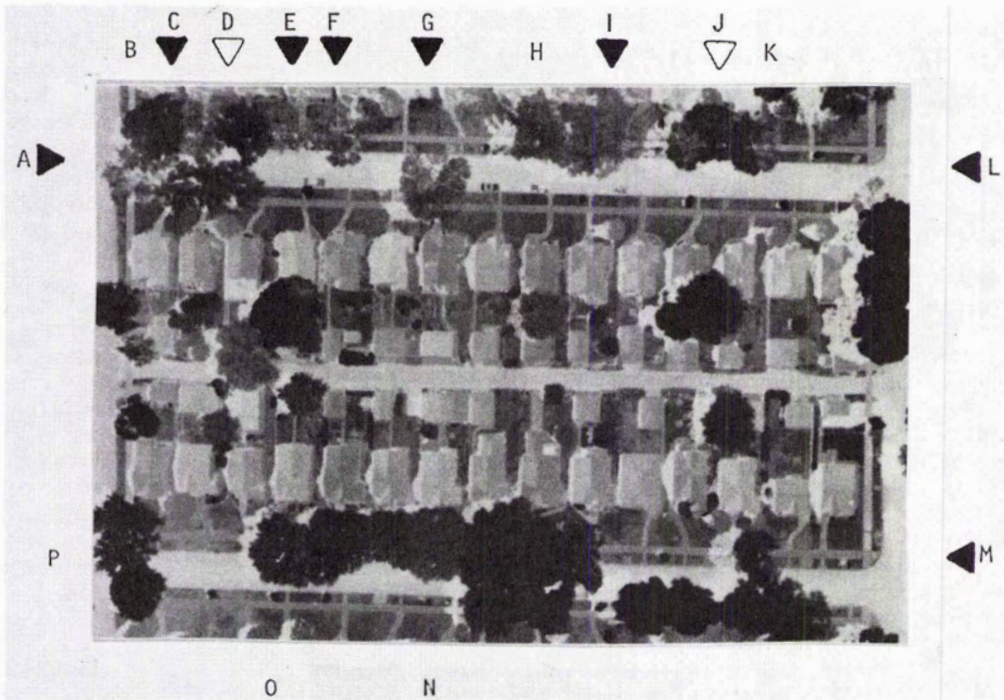
(a)



(b)



(c)



(d)

FIG. 1. Sample ratio and discriminant images. (a) Green/infrared ratio. (b) Red/infrared ratio. (c) Green/red ratio. (d) Multiple discriminant image.

similarity between these three images indicates the high correlation between the green and red reflectance data found in the tree crown. Another effect of the green-red correlation is the noisy appearance of the green/red ratio (Figure 1c). Because this ratio shows differences between the essentially equivalent green and red bands, a small range of values resulted. Contrast stretching of the data caused the small, correlated differences to be greatly exaggerated. The result was not found to be useful.

The ability to classify trees on the basis of enhanced image tone simplifies the interpretation process, but errors still occur. For example, crowns *H* and *I* have the same appearance on the ratio and discriminant images in spite of one being healthy (*H*) and one being diseased (*I*). Also, in this case, the color contrast stretch image vividly indicates the disease. Note also that diseased crowns *D* and *M* appear healthy on the ratio and discriminant images.

The ratio images certainly do not make the interpretation process an "automatic" procedure. On crowns with discrete patches of diseased branches, only the patches appear light (see *J*). Sparse crowns, such as *L*, are even more difficult to identify on such images.

An interesting effect also illustrated in Figure 1 is the incomplete reduction of the shading influence in the images (best seen on the house roofs). The incomplete removal of the shade effect is indicative of the slightly spectral nature of shade. Rather than being equally reduced across the spectrum, the brightness in shaded areas is reduced as a function of wavelength and this spectral difference is indicated by the slight tonal variations within uniform features on the ratio images.

INTERPRETATION PROCEDURE AND RESULTS

Interpretation of the enhancements was performed by Interpreter 2 (Interpreter 1 was unavailable at the time of this activity). The 1:12,000 contrast stretched photos were interpreted for D^1 and D^2 classes (high and moderate confidence in the detection of DED). The D^3 class was omitted due to the lack of success with it in the earlier analyses. A representative subset of the entire study area was used for the detailed analysis of the enhancements.

The interpretation of the contrast stretched images was performed on first generation positive transparencies. Both positives and negatives had been produced on the film recorder, and color enlargements were prepared from the negative. While useful for annotation, the prints were found to lack the color fidelity and spatial resolution of the first generation positive transparencies. The square shape of individual pixels in the 1100 by 1100 grid could readily be seen on the positive transparency, but not on the prints. Due to the

small size of the transparencies (the Dicomed image recorder uses 4- by 5-inch film) the interpretation was done under $2\times$ to $4\times$ magnification.

In addition to the contrast stretch image, one of the ratio images was interpreted in detail. The green/infrared ratio was chosen after preliminary evaluation indicated it was the most interpretable. Again, the 1:12,000 original scale data were used.

At this stage in the study, the multiple discriminant analysis procedure was still under development, and images were not available until later. When these products became available, analysis revealed their essential equivalence to the ratio data (as shown in Figure 1). Accordingly, a repeated interpretation of this image did not appear to be necessary.

Table 2a summarizes the results of the interpretation of the enhancements. The "original photography" table was extracted from the Interpreter 2 analysis done previously for the limited geographical subset area of the enhancement test. Table 2b lists the corresponding accuracy and error rates. The results show an improvement in errors of omission and commission for the contrast stretch interpretation, and a further reduction in commission errors, with lower accuracy, for the ratio interpretation.

CONCLUSIONS

The results of this study have indicated an improvement in interpretation accuracy can be realized with the use of digitally enhanced imagery. These improvements are not, however, on a large order of magnitude considering the added expense of the digital processing. Nor do they offer sufficient improvement in accuracy to offer a viable alternative or complement to the ground survey process for DED control.

The digital techniques were found to increase dramatically the visual expression of crown color variations. The problem is the inconsistency with which these variations indicate DED. Some diseased trees have manifestations on lower branches only, presenting a healthy crown to the aerial camera. No amount of enhancement will enable correct interpretation of these crowns on vertical photography. Conversely, healthy crowns having slight color variations due to other causes may be interpreted as diseased after the enhancement process amplifies the variations. In short, the *inconsistency* of the manifestations of DED is a problem in addition to their subtlety. When applied to detection of tree (and agricultural crop) stresses having more consistent spectral manifestation, it appears that the digital processing approach developed in this study is very effective. Applied to DED, it unfortunately is not.

The specific conclusions drawn under the conditions of this study are listed below.

TABLE 2. RESULTS OF ENHANCED IMAGERY INTERPRETATION TEST

		GROUND DATA		
		healthy	diseased	
PHOTOINTERPRETED DATA	A. Original photography	healthy	349	12
		diseased	$\frac{D^2}{D^1}$	$\frac{43}{1}$
	B. Contrast Stretch	healthy	352	10
		diseased	$\frac{D^2}{D^1}$	$\frac{19}{22}$
	C. Ratio (green/ir)	healthy	360	12
		diseased	$\frac{D^2}{D^2}$	$\frac{19}{14}$
	total:		393	34

(b) Accuracy and errors

	ACCURACY	ERRORS	
		omission	commission
A. Original Photography	$\frac{22}{34} = 65\%$	$\frac{12}{34} = 35\%$	$\frac{44}{34} = 129\%$
B. Contrast Stretch	$\frac{24}{34} = 71\%$	$\frac{10}{34} = 29\%$	$\frac{41}{34} = 121\%$
C. Ratio (green/ir)	$\frac{22}{34} = 65\%$	$\frac{12}{34} = 35\%$	$\frac{33}{34} = 97\%$

- Initial identification of elm trees was most easily performed on the May "leaf-off" photography. The characteristic color, branching, and early foliage made distinction of the elm crowns possible, and the lack of dense foliage aided in the differentiation of closely spaced trees for base mapping purposes.
- A mid-season (25 July) date of photography provided the best interpretation. Early season photographs were more difficult to use due to effects of a canker worm outbreak in our study period. Late season photography had excessive shadows due to the lower sun angle. (The optimum date of detection will vary with the conditions in any given season and study area.)
- Interpreters of the original photography preferred 1:6,000 over 1:12,000 scale. The larger scale improved the interpretation of crown shape and condition but limited areal coverage per frame. A scale of 1:10,000 represents a reasonable compromise between coverage and detail.

- The accuracy of conventional interpretation applied to DED detection is highly variable, depending on the experience and bias of the interpreter. This points to the need for thorough training of interpreters prior to any attempt to detect the disease photographically.
- The digital enhancements dramatically improved the visual expression of crown color variations. The factors of crown shape and condition were more difficult to analyze due to a slight loss of spatial detail on the digital imagery. At the same time, background effects (where the ground shows through the crown) were reduced by spatially integrated nature of the digital imagery, especially on the 1:12,000 scale images which were preferred by the interpreter.
- Analysis of ratio images showed the red/infrared and green/infrared combinations to be useful and nearly equivalent. The green/red combination was not useful. A multivariate discriminant analysis was also used to transform the data. Results were very similar to the two ratio products. Because of this result, and considering the extra effort required, the discriminant analysis was not effective in this application.
- Test results indicated improved accuracy with the contrast stretch and green/infrared ratio images compared to the original photography. The improvement is not, however, large enough to warrant the cost of digital processing, nor are the accuracies high enough for the data to be of practical value.
- The problems encountered in detecting DED accurately with the digital data seem to be largely due to the characteristics of the disease. Again, the digital techniques employed have been found to be extremely effective when applied to tree and plant stresses having more consistent spectral manifestations. Further research in this direction is suggested.

ACKNOWLEDGMENTS

The scanning microdensitometer data used in this study were obtained through the cooperation of the Environmental Remote Sensing Center at the University of Wisconsin-Madison. Ground data were provided through the courtesy of the municipalities of Lauderdale, Falcon Heights, and St. Paul, Minnesota. University personnel assisting in the acquisition of ground data included Mark Stennes and Katherine J. Zuzek. The aerial photography used in this study was taken by Phillip D. Grumstrup, Mark A. Springan, and Lee M. Westfield. The manual image interpretation and computer processing procedures were performed with the assistance of Stephen C. Bernath and Roy T. Hagen. Anne LaMois Downs, Katherine A. Knutson, and Clara M. Schreiber assisted in the production of this manuscript. Many aspects of this study were supported directly or indirectly by funding from the University of Minnesota College of Forestry and Agricultural Experiment Station (Proj. MIN-42-033 and 038).

REFERENCES

- Fairweather, S. E., *et al.*, 1978. The use of CIR aerial photography for Dutch elm disease, *Proceedings: Symposium on Remote Sensing for Vegetation Damage Assessment*. pp. 229-310
- French, D. W., and M. P. Meyer, 1969. Aerial survey for oak wilt and Dutch elm disease in Bloomington, Minnesota, *Proceedings: Workshop on Aerial Color Photography in the Plant Sciences*. University of Florida, Gainesville, Florida. pp. 77-80
- French, D. W., *et al.*, 1974. *Remote sensing applications to the management of agricultural, forest and water resources in Minnesota*. IAFHE RSL Res. Rept. 74-2. Annual Progress Report NASA Grant NGL 24-005-263. 57 p.
- Hammerschlag, R. S., and W. J. Sopstyle, 1975. Investigations of remote sensing techniques for early detection of Dutch elm disease, *Proceedings: Fourth Annual Remote Sensing of Earth Resources Conference*, Tullahoma, Tennessee. pp. 357-386.
- Lillesand, T. M., *et al.*, 1979. Quantifying urban tree stress through microdensitometric analysis of aerial photography, *Photogrammetric Engineering and Remote Sensing*, Vol. 45, No. 10. pp. 1401-1410.
- Lillesand, T. M., and R. W. Kiefer, 1979. *Remote Sensing and Image Interpretation*, John Wiley & Sons, New York. 612 p.
- Lillesand, T. M., and D. E. Meisner, 1981. Application of scanning microdensitometer data in selected plant science case studies, *Proceedings: Workshop on Color Aerial Photography in the Plant Sciences*. Luray, Virginia. 12 p., in press.
- Meyer, M. P., and D. W. French, 1967. Detection of diseased trees, *Photogrammetric Engineering*, 33:1, pp. 1035-1040.
- Morrison, D. F., 1976. *Multivariate Statistical Methods*, McGraw-Hill. pp. 128-345.
- Nash, M. R., *et al.*, 1977. *Detection of Dutch elm disease using oblique 35 mm aerial photography*, IAFHE RSL Res. Rept. 77-9, 16 p.
- Stevens, A. R., 1972. *Application of color and color infrared aerial photography to Dutch elm disease detection*, A Doctoral Dissertation, University of Wisconsin Department of Civil and Environmental Engineering, Madison, Wisconsin, 150 p.

(Received 14 October 1980; accepted 23 March 1981; revised 23 June 1981)

Second Winter Institute in Surveying Engineering

University of Maine at Orono
11-15 January 1982

This year's Institute deals with "Theory and Practice of Least Squares Adjustments in Surveying and Photogrammetry." A carefully selected balance of lectures, step-by-step discussion of laboratories, and actual computations on the computer using a prepared program package will lead to a comprehensive understanding of the use of adjustments and to a systematic approach in formulating, setting-up, and analyzing adjustments. The following topics will be discussed: stochastic models, mathematical models, iterations, parameterization, conditions between parameters, sequential solutions, techniques for detecting blunders, variance-covariance propagation, statistical tests, general linear hypothesis, motion analysis, simulation, optimization, mathematical evaluation of evidence, minimal and inner constraint solutions, and the role of coordinates and error ellipses in two-dimensional networks.

Track 1 will deal in greater detail with applications in surveying. Track 2 will concentrate on applications in photogrammetry.

Throughout the Institute the participants can use a prepared adjustment package which is implemented on the main frame computer and the microcomputer. All evenings will be available for laboratory work and for study of nearly 100 sample adjustments which are part of the lecture notes.

The tuition fee, which includes refreshments, lunch, dinner, and lecture notes, is \$500.

For further information please contact

Prof. Alfred Leick
Department of Civil Engineering
University of Maine at Orono
Orono, ME 04469
Tele. (207) 581-2561